343. Investigation of Compression of Packages

A. Kabelkaitė[1], E. Kibirkštis[1], L. Ragulskis[2]
[1] Kaunas University of Technology,
Studentų 56-350, LT-51424 Kaunas, Lithuania,
Phone: (8 37) 300 237,
E-mail: *asta.kabelkaite@ktu.lt, edmundas.kibirkstis@ktu.lt*
[2] Vytautas Magnus University,
Vileikos 8-702, LT-44404 Kaunas, Lithuania,
E-mail: *l.ragulskis@if.vdu.lt*

(Received 6 January 2008; accepted 17 March 2008)

Abstract. The model for the analysis of compression of a long structure with a constant thin-walled cross-section is presented. It is assumed that a structure experiences static compression and the problem of initial stability for a cross-section is solved.

The analysis of compression of a shell-type structure is described assuming that a structure undergoes static compression and the problem of initial stability is solved.

The results of experimental investigation of resistance to compression of paperboard packages are presented for different grammage of the materials of paperboard and for the machine and cross-machine directions of production of paperboard. The largest permissible vertical pressure load that the packages are able to resist is determined.

Keywords: cross-section, thin-walled, compression, stability, eigenmode, finite elements, shell, paperboard, packages, experimental setup.

Introduction

In recent years the research of mechanical characteristics and materials of packages are of increasing importance, particularly when the research is devoted to the optimization of geometrical and strength parameters of the packages by taking into account mechanical resistance to vibrations, impacts and static loads.

The analysis of stability of packages is based on the relationships described in [1].

Some results of experimental investigation of compression of packages are presented in reference [2].

Stability of a long structure with a constant thin-walled cross-section affected by the additional stiffness due to the static compression is studied in this paper (the first stability eigenmodes are determined).

The analysis of stability of a shell-type structure consists of two stages:

1) static problem is solved by assuming that the displacements at the edges of the structure are given;
2) stability of the structure is investigated since the structure is subjected to the additional stiffness induced by the static compression that was determined in the previous stage.

Model for the analysis of stability of a long structure with a constant thin-walled cross-section

Further x, y and z denote the axes of the orthogonal Cartesian system of coordinates. It is assumed that the structure looses stability according to the first harmonic in the longitudinal direction.

It is assumed that:

$$u(x,y,z) = \bar{u}(x,y)\sin\frac{\pi z}{L}, \quad (1)$$

$$v(x,y,z) = \bar{v}(x,y)\sin\frac{\pi z}{L}, \quad (2)$$

$$w(x,y,z) = \bar{w}(x,y)\cos\frac{\pi z}{L}, \quad (3)$$

where u, v and w are the displacements in the directions of the orthogonal Cartesian system of coordinates and the upper dash indicates the amplitude of the first harmonic of the displacements, while L is the length of the structure.

The following matrixes are introduced:

$$\begin{bmatrix} [N_u] \\ [N_v] \\ [N_w] \end{bmatrix} = \begin{bmatrix} N_1 & 0 & 0 & \dots \\ 0 & N_1 & 0 & \dots \\ 0 & 0 & N_1 & \dots \end{bmatrix}, \quad (4)$$

$$\begin{bmatrix} [N_{ux}] \\ [N_{vx}] \\ [N_{wx}] \end{bmatrix} = \begin{bmatrix} \frac{\partial N_1}{\partial x} & 0 & 0 & \dots \\ 0 & \frac{\partial N_1}{\partial x} & 0 & \dots \\ 0 & 0 & \frac{\partial N_1}{\partial x} & \dots \end{bmatrix}, \quad (5)$$

$$\begin{bmatrix} [N_{uy}] \\ [N_{vy}] \\ [N_{wy}] \end{bmatrix} = \begin{bmatrix} \frac{\partial N_1}{\partial y} & 0 & 0 & \dots \\ 0 & \frac{\partial N_1}{\partial y} & 0 & \dots \\ 0 & 0 & \frac{\partial N_1}{\partial y} & \dots \end{bmatrix}, \quad (6)$$

where N_i are the shape functions of the analyzed finite element.

The stiffness matrix is expressed as:

$$[K] = \int \left([B_s]^T [D][B_s] + [B_c]^T [D][B_c] \right) dxdy, \quad (7)$$

where:

$$[D] = \begin{bmatrix} \bar{K} & \tilde{K} & \tilde{K} & 0 & 0 & 0 \\ \tilde{K} & \bar{K} & \tilde{K} & 0 & 0 & 0 \\ \tilde{K} & \tilde{K} & \bar{K} & 0 & 0 & 0 \\ 0 & 0 & 0 & G & 0 & 0 \\ 0 & 0 & 0 & 0 & G & 0 \\ 0 & 0 & 0 & 0 & 0 & G \end{bmatrix}, \quad (8)$$

where:

$$\bar{K} = K + \frac{4}{3} G, \quad (9)$$

$$\tilde{K} = K - \frac{2}{3} G, \quad (10)$$

$$K = \frac{E}{3(1-2\nu)}, \quad (11)$$

$$G = \frac{E}{2(1+\nu)}, \quad (12)$$

where E is the modulus of elasticity and ν is the Poisson's ratio. The matrixes $[B_s]$ and $[B_c]$ are defined from:

$$\begin{aligned} \{\varepsilon(x,y,z)\} &= [B_s(x,y)]\{\delta\} \sin \frac{\pi z}{L} + \\ &+ [B_c(x,y)]\{\delta\} \cos \frac{\pi z}{L}, \end{aligned} \quad (13)$$

where $\{\varepsilon\}$ is the vector of strains, $\{\delta\}$ is the nodal displacement vector and:

$$[B_s] = \begin{bmatrix} [N_{ux}] \\ [N_{vy}] \\ -[N_w]\frac{\pi}{L} \\ [N_{uy}] + [N_{vx}] \\ [0] \\ [0] \end{bmatrix}, \quad (14)$$

$$[B_c] = \begin{bmatrix} [0] \\ [0] \\ [0] \\ [0] \\ [N_v]\frac{\pi}{L} + [N_{wy}] \\ [N_u]\frac{\pi}{L} + [N_{wx}] \end{bmatrix}. \quad (15)$$

The structure is assumed to be statically compressed as a bar and thus the static displacement is:

$$w = -z. \quad (16)$$

This gives the strain:

$$\varepsilon_z = -1. \quad (17)$$

For a thin-walled cross-section the stress is expressed as:

$$\sigma_z = -\frac{E}{1-\nu^2}. \quad (18)$$

The matrix of additional stiffness has the following form:

$$[K_\sigma] = \int \left(\begin{gathered} [G_s]^T \left(-\frac{E}{1-\nu^2} \right) [G_s] + \\ + [G_c]^T \left(-\frac{E}{1-\nu^2} \right) [G_c] \end{gathered} \right) dxdy, \quad (19)$$

where $[G_s]$ and $[G_c]$ are defined from the following relationship:

$$\begin{Bmatrix} \dfrac{\partial u(x,y,z)}{\partial z} \\ \dfrac{\partial v(x,y,z)}{\partial z} \\ \dfrac{\partial w(x,y,z)}{\partial z} \end{Bmatrix} = [G_S(x,y)]\{\delta\}\sin\frac{\pi z}{L} + \tag{20}$$

$$+[G_C(x,y)]\{\delta\}\cos\frac{\pi z}{L},$$

where:

$$[G_S] = \begin{bmatrix} [0] \\ [0] \\ -[N_w]\dfrac{\pi}{L} \end{bmatrix}, \tag{21}$$

$$[G_C] = \begin{bmatrix} [N_u]\dfrac{\pi}{L} \\ [N_v]\dfrac{\pi}{L} \\ [0] \end{bmatrix}. \tag{22}$$

Results of analysis of stability of a long structure with a constant thin-walled cross-section

A long structure with a square cross-section is analyzed. The cross-section when $z = \dfrac{L}{2}$ for the first eigenmode of stability is presented in Fig. 1, for the second eigenmode of stability is presented in Fig. 2, … , for the ninth eigenmode of stability is presented in Fig. 9. The first and the second eigenmodes correspond to the same eigenvalue, as well as the seventh and the eighth eigenmodes correspond to the same eigenvalue.

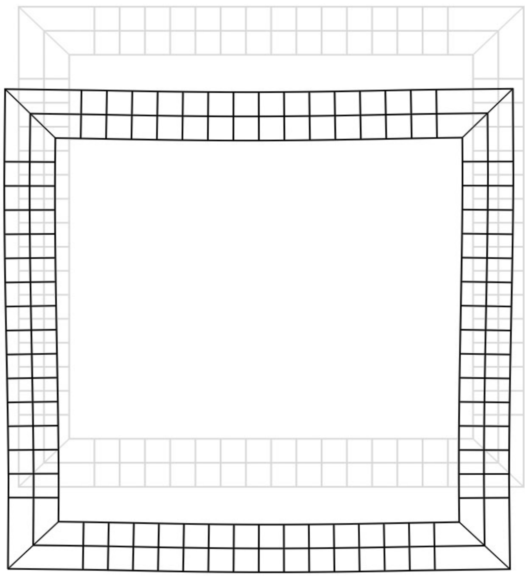

Fig. 1. The first stability eigenmode

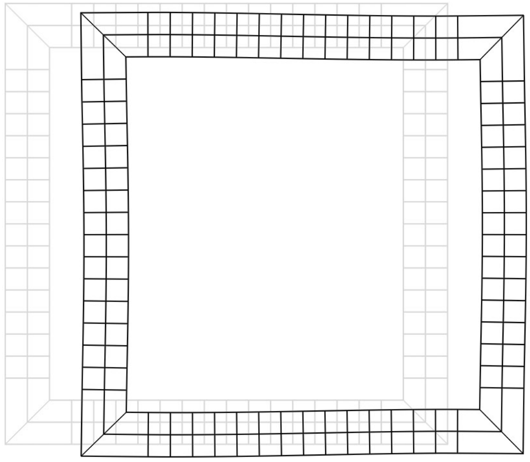

Fig. 2. The second stability eigenmode

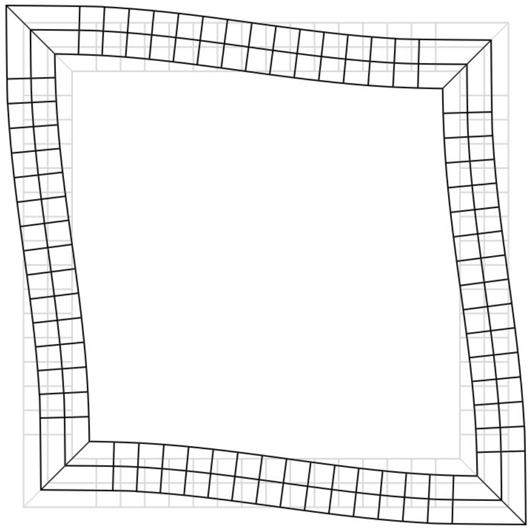

Fig. 3. The third stability eigenmode

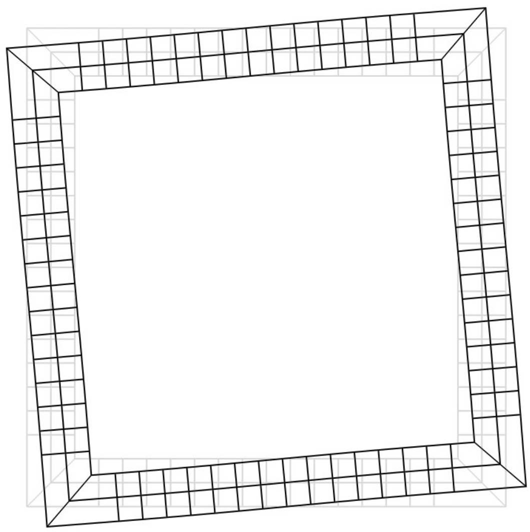

Fig. 4. The fourth stability eigenmode.

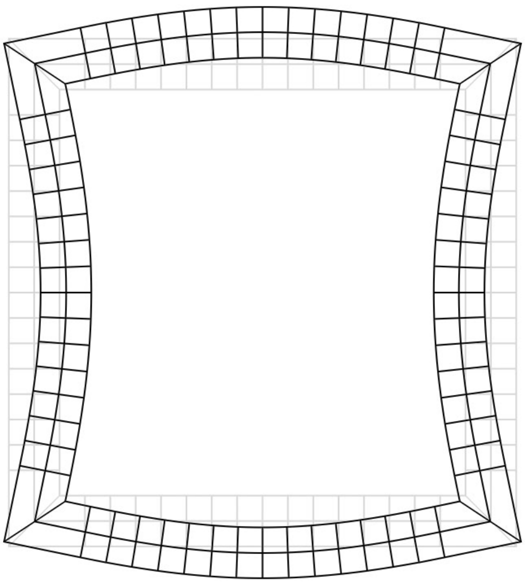

Fig. 5. The fifth stability eigenmode

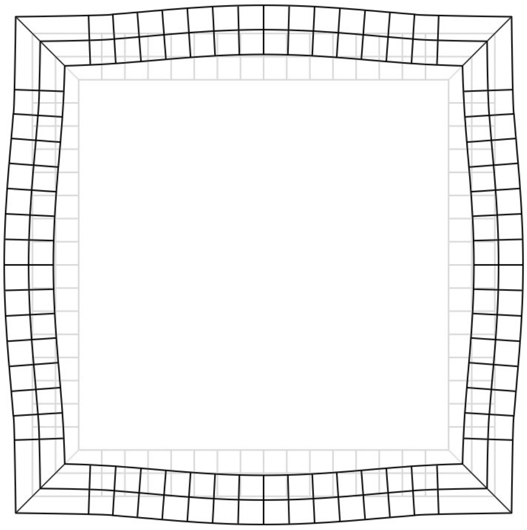

Fig. 6. The sixth stability eigenmode

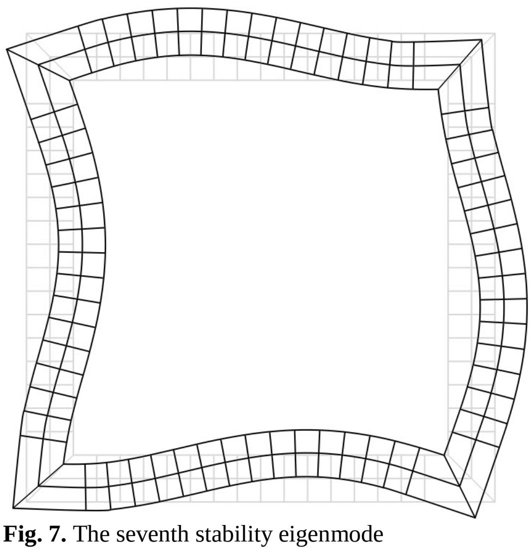

Fig. 7. The seventh stability eigenmode

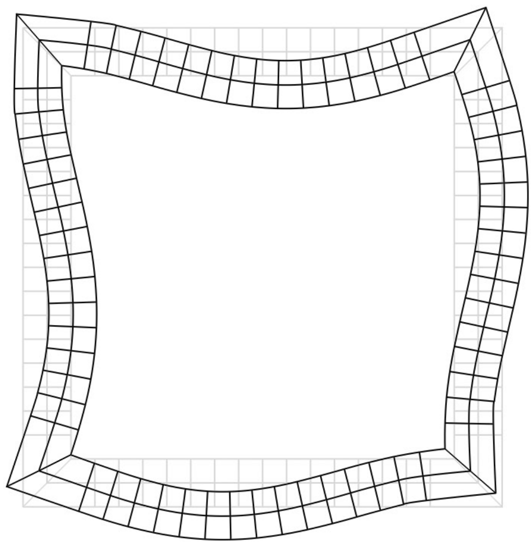

Fig. 8. The eighth stability eigenmode

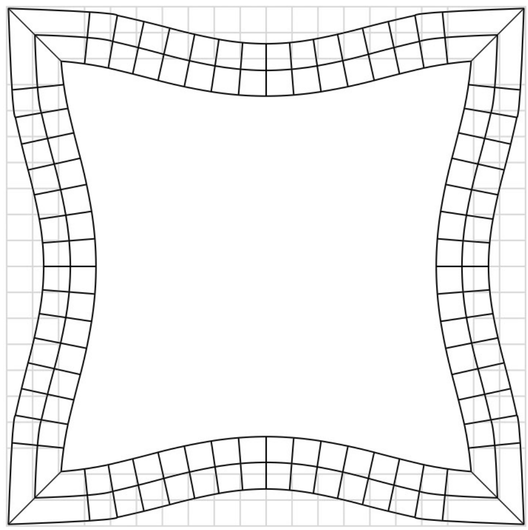

Fig. 9. The ninth stability eigenmode

Model for the analysis of stability of the shell-type structure

First the static problem is analyzed. The element has six nodal degrees of freedom, they are the displacements of the lower surface of the shell in the directions of the axes x, y and z and the displacements of the upper surface of the shell in the directions of the axes x, y and z.

It is assumed that the displacements at the boundary of the analyzed structure are given and they produce the loading vector. Thus the vector of displacements $\{\delta\}$ is determined by solving the system of linear algebraic equations.

In the second stage of the analysis the eigenproblem of stability of the structure with additional stiffness due to the static compression is solved.

The derivatives of x, y and z with respect to the local coordinates ξ and η are calculated as:

$$\begin{bmatrix} \frac{\partial x}{\partial \xi} & \frac{\partial y}{\partial \xi} & \frac{\partial z}{\partial \xi} \\ \frac{\partial x}{\partial \eta} & \frac{\partial y}{\partial \eta} & \frac{\partial z}{\partial \eta} \end{bmatrix} = \begin{bmatrix} \frac{\partial N_1}{\partial \xi} & \frac{\partial N_2}{\partial \xi} & \ldots \\ \frac{\partial N_1}{\partial \eta} & \frac{\partial N_2}{\partial \eta} & \ldots \end{bmatrix} \cdot \begin{bmatrix} x_1 & y_1 & z_1 \\ x_2 & y_2 & z_2 \\ \vdots & \vdots & \vdots \end{bmatrix}, \tag{23}$$

where x_i, y_i, z_i are the nodal coordinates of the finite element. The vector $\begin{Bmatrix} n_x \\ n_y \\ n_z \end{Bmatrix}$ is the unit vector in the direction of the vector product of $\begin{Bmatrix} \frac{\partial x}{\partial \xi} \\ \frac{\partial y}{\partial \xi} \\ \frac{\partial z}{\partial \xi} \end{Bmatrix}$ and $\begin{Bmatrix} \frac{\partial x}{\partial \eta} \\ \frac{\partial y}{\partial \eta} \\ \frac{\partial z}{\partial \eta} \end{Bmatrix}$. The vector $\begin{Bmatrix} r_x \\ r_y \\ r_z \end{Bmatrix}$ is the unit vector in the direction of the vector $\begin{Bmatrix} \frac{\partial x}{\partial \xi} \\ \frac{\partial y}{\partial \xi} \\ \frac{\partial z}{\partial \xi} \end{Bmatrix}$. The vector $\begin{Bmatrix} t_x \\ t_y \\ t_z \end{Bmatrix}$ is the vector product of $\begin{Bmatrix} n_x \\ n_y \\ n_z \end{Bmatrix}$ and $\begin{Bmatrix} r_x \\ r_y \\ r_z \end{Bmatrix}$. The Jacobian is calculated as:

$$[J] = \begin{bmatrix} \frac{\partial x}{\partial \xi} & \frac{\partial y}{\partial \xi} & \frac{\partial z}{\partial \xi} \\ \frac{\partial x}{\partial \eta} & \frac{\partial y}{\partial \eta} & \frac{\partial z}{\partial \eta} \end{bmatrix} \begin{bmatrix} r_x & t_x \\ r_y & t_y \\ r_z & t_z \end{bmatrix}. \tag{24}$$

The following matrixes are introduced:

$$\begin{bmatrix} [\overline{N}_u] \\ [\overline{N}_v] \\ [\overline{N}_w] \end{bmatrix} = [T] \begin{bmatrix} N_1 & 0 & 0 & 0 & 0 & 0 & \ldots \\ 0 & N_1 & 0 & 0 & 0 & 0 & \ldots \\ 0 & 0 & N_1 & 0 & 0 & 0 & \ldots \end{bmatrix}, \tag{25}$$

$$\begin{bmatrix} [\overline{\overline{N}}_u] \\ [\overline{\overline{N}}_v] \\ [\overline{\overline{N}}_w] \end{bmatrix} = [T] \begin{bmatrix} 0 & 0 & 0 & N_1 & 0 & 0 & \ldots \\ 0 & 0 & 0 & 0 & N_1 & 0 & \ldots \\ 0 & 0 & 0 & 0 & 0 & N_1 & \ldots \end{bmatrix}, \tag{26}$$

$$\begin{bmatrix} [\overline{N}_{ur}] \\ [\overline{N}_{vr}] \\ [\overline{N}_{wr}] \end{bmatrix} = [T] \begin{bmatrix} \frac{\partial N_1}{\partial r} & 0 & 0 & 0 & 0 & 0 & \ldots \\ 0 & \frac{\partial N_1}{\partial r} & 0 & 0 & 0 & 0 & \ldots \\ 0 & 0 & \frac{\partial N_1}{\partial r} & 0 & 0 & 0 & \ldots \end{bmatrix}, \tag{27}$$

$$\begin{bmatrix} [\overline{\overline{N}}_{ur}] \\ [\overline{\overline{N}}_{vr}] \\ [\overline{\overline{N}}_{wr}] \end{bmatrix} = [T] \begin{bmatrix} 0 & 0 & 0 & \frac{\partial N_1}{\partial r} & 0 & 0 & \ldots \\ 0 & 0 & 0 & 0 & \frac{\partial N_1}{\partial r} & 0 & \ldots \\ 0 & 0 & 0 & 0 & 0 & \frac{\partial N_1}{\partial r} & \ldots \end{bmatrix}, \tag{28}$$

$$\begin{bmatrix} [\overline{N}_{ut}] \\ [\overline{N}_{vt}] \\ [\overline{N}_{wt}] \end{bmatrix} = [T] \begin{bmatrix} \frac{\partial N_1}{\partial t} & 0 & 0 & 0 & 0 & 0 & \ldots \\ 0 & \frac{\partial N_1}{\partial t} & 0 & 0 & 0 & 0 & \ldots \\ 0 & 0 & \frac{\partial N_1}{\partial t} & 0 & 0 & 0 & \ldots \end{bmatrix}, \tag{29}$$

$$\begin{bmatrix} [\overline{\overline{N}}_{ut}] \\ [\overline{\overline{N}}_{vt}] \\ [\overline{\overline{N}}_{wt}] \end{bmatrix} = [T] \begin{bmatrix} 0 & 0 & 0 & \frac{\partial N_1}{\partial t} & 0 & 0 & \ldots \\ 0 & 0 & 0 & 0 & \frac{\partial N_1}{\partial t} & 0 & \ldots \\ 0 & 0 & 0 & 0 & 0 & \frac{\partial N_1}{\partial t} & \ldots \end{bmatrix}, \tag{30}$$

where:

$$[T] = \begin{bmatrix} r_x & r_y & r_z \\ t_x & t_y & t_z \\ n_x & n_y & n_z \end{bmatrix}. \tag{31}$$

The displacements u, v, w in the directions of the local axes on the surface of the shell can be represented in the following way:

$$u = \frac{H-n}{H}[\overline{N}_u]\{\delta\} + \frac{n}{H}[\overline{\overline{N}}_u]\{\delta\}, \tag{32}$$

$$v = \frac{H-n}{H}[\overline{N}_v]\{\delta\} + \frac{n}{H}[\overline{\overline{N}}_v]\{\delta\}, \tag{33}$$

$$w = \frac{H-n}{H}[\overline{N}_w]\{\delta\} + \frac{n}{H}[\overline{\overline{N}}_w]\{\delta\}, \tag{34}$$

where H is the thickness of the shell and n is the coordinate in the normal direction to the surface of the shell (n=0 corresponds to the lower surface and n=H corresponds to the upper surface).

The strains are expressed as:

$$\{\varepsilon\}=\frac{1}{H}[B]\{\delta\}+\frac{H-n}{H}[\overline{B}]\{\delta\}+\frac{n}{H}[\overline{\overline{B}}]\{\delta\}, \quad (35)$$

where:

$$[B]=\begin{bmatrix}[0]\\ [0]\\ [\overline{\overline{N}}_w]-[\overline{N}_w]\\ [0]\\ [\overline{\overline{N}}_v]-[\overline{N}_v]\\ [\overline{\overline{N}}_u]-[\overline{N}_u]\end{bmatrix}, \quad (36)$$

$$[\overline{B}]=\begin{bmatrix}[\overline{N}_{ur}]\\ [\overline{N}_{vt}]\\ [0]\\ [\overline{N}_{ut}]+[\overline{N}_{vr}]\\ [\overline{N}_{wt}]\\ [\overline{N}_{wr}]\end{bmatrix}, \quad (37)$$

$$[\overline{\overline{B}}]=\begin{bmatrix}[\overline{\overline{N}}_{ur}]\\ [\overline{\overline{N}}_{vt}]\\ [0]\\ [\overline{\overline{N}}_{ut}]+[\overline{\overline{N}}_{vr}]\\ [\overline{\overline{N}}_{wt}]\\ [\overline{\overline{N}}_{wr}]\end{bmatrix}. \quad (38)$$

The stiffness matrix has the form:

$$[K]=$$
$$=\int\left(\begin{array}{l}[B]^T[D]\frac{1}{2}[\overline{B}]+[\overline{B}]^T[D]\frac{1}{2}[B]+\\ +[B]^T[D]\frac{1}{2}[\overline{\overline{B}}]+[\overline{\overline{B}}]^T[D]\frac{1}{2}[B]+\\ +[\overline{B}]^T[D]\frac{H}{6}[\overline{\overline{B}}]+[\overline{\overline{B}}]^T[D]\frac{H}{6}[\overline{B}]+\\ +[\overline{B}]^T[D]\frac{H}{3}[\overline{B}]+[\overline{\overline{B}}]^T[D]\frac{H}{3}[\overline{\overline{B}}]+\\ +[B]^T[D]\frac{1}{H}[B]\end{array}\right)drdt, \quad (39)$$

where:

$$[D]=\begin{bmatrix}\overline{K} & \tilde{K} & \tilde{K} & 0 & 0 & 0\\ \tilde{K} & \overline{K} & \tilde{K} & 0 & 0 & 0\\ \tilde{K} & \tilde{K} & \overline{K} & 0 & 0 & 0\\ 0 & 0 & 0 & G & 0 & 0\\ 0 & 0 & 0 & 0 & \frac{G}{1.2} & 0\\ 0 & 0 & 0 & 0 & 0 & \frac{G}{1.2}\end{bmatrix}. \quad (40)$$

Also the following integrals have been taken into account:

$$\int_0^H \frac{1}{H}\frac{H-n}{H}dn=\int_0^H \frac{1}{H}\frac{n}{H}dn=\frac{1}{2}, \quad (41)$$

$$\int_0^H \frac{H-n}{H}\frac{n}{H}dn=\frac{H}{6}, \quad (42)$$

$$\int_0^H \left(\frac{H-n}{H}\right)^2 dn=\int_0^H \left(\frac{n}{H}\right)^2 dn=\frac{H}{3}, \quad (43)$$

$$\int_0^H \left(\frac{1}{H}\right)^2 dn=\frac{1}{H}. \quad (44)$$

The derivatives of the transverse displacement with respect to the tangential coordinates are expressed as:

$$\begin{Bmatrix}\frac{\partial w}{\partial r}\\ \frac{\partial w}{\partial t}\end{Bmatrix}=\frac{H-n}{H}[\overline{G}]\{\delta\}+\frac{n}{H}[\overline{\overline{G}}]\{\delta\}, \quad (45)$$

where:

$$[\overline{G}]=\begin{bmatrix}[\overline{N}_{wr}]\\ [\overline{N}_{wt}]\end{bmatrix}, \quad (46)$$

$$[\overline{\overline{G}}]=\begin{bmatrix}[\overline{\overline{N}}_{wr}]\\ [\overline{\overline{N}}_{wt}]\end{bmatrix}. \quad (47)$$

The stresses in the middle surface of the shell are determined from the static problem:

$$\begin{Bmatrix}\sigma_r\\ \sigma_t\\ \sigma_n\\ \tau_{rt}\\ \tau_{tn}\\ \tau_{rn}\end{Bmatrix}=[D]\left(\frac{1}{H}[B]+\frac{1}{2}[\overline{B}]+\frac{1}{2}[\overline{\overline{B}}]\right)\{\delta\}. \quad (48)$$

The matrix of stresses has the following form:

$$[M]=\begin{bmatrix}\sigma_r & \tau_{rt}\\ \tau_{rt} & \sigma_t\end{bmatrix}. \quad (49)$$

The matrix of additional stiffness has the form:

$$[K_\sigma]= \\ =\int\begin{pmatrix}[\overline{G}]^T[M]\dfrac{H}{6}[\overline{\overline{G}}]+[\overline{\overline{G}}]^T[M]\dfrac{H}{6}[\overline{G}]+ \\ +[\overline{G}]^T[M]\dfrac{H}{3}[\overline{G}]+[\overline{\overline{G}}]^T[M]\dfrac{H}{3}[\overline{\overline{G}}]\end{pmatrix}drdt. \qquad (50)$$

Results of analysis of stability of the shell-type structure

A structure that is square in the *xy* plane and the initial geometry of which does not change in the *z* direction is analyzed. For the static problem the following boundary conditions are assumed: on the lower boundary all the displacements are equal to 0, on the upper boundary all the displacements are equal to 0 except for the displacement in the direction of the *z* axis which is equal to -1. For the eigenproblem on the lower and the upper boundaries all the displacements are assumed to be equal to zero.

The first eigenmode of stability is presented in Fig. 10, the second eigenmode of stability is presented in Fig. 11, … , the eighth eigenmode of stability is presented in Fig. 17. The first and the second eigenmodes correspond to the same eigenvalue. The fifth and the sixth eigenmodes correspond to the same eigenvalue.

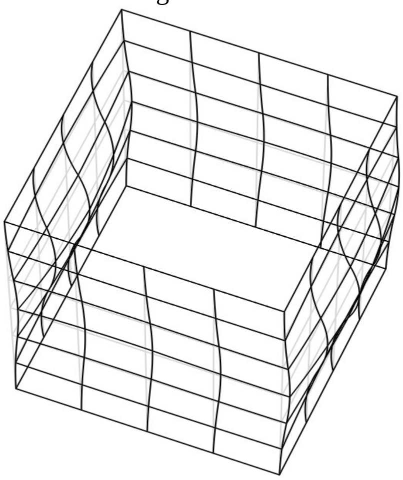

Fig. 10. The first stability eigenmode

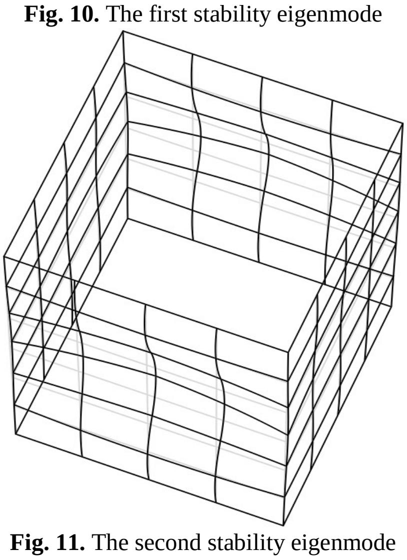

Fig. 11. The second stability eigenmode

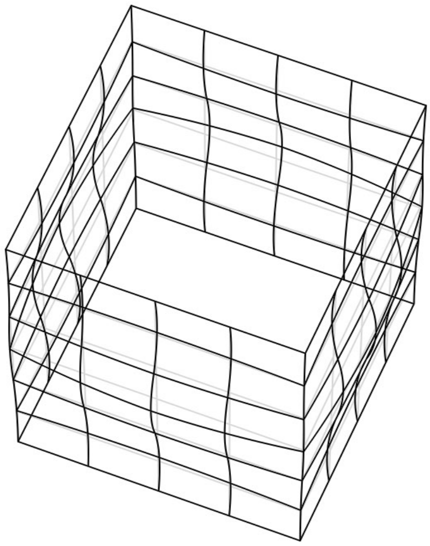

Fig. 12. The third stability eigenmode

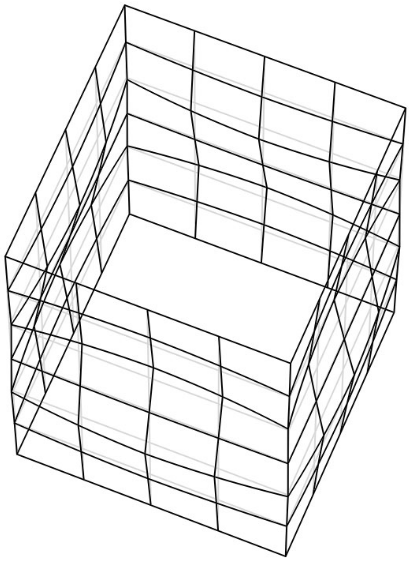

Fig. 13. The fourth stability eigenmode

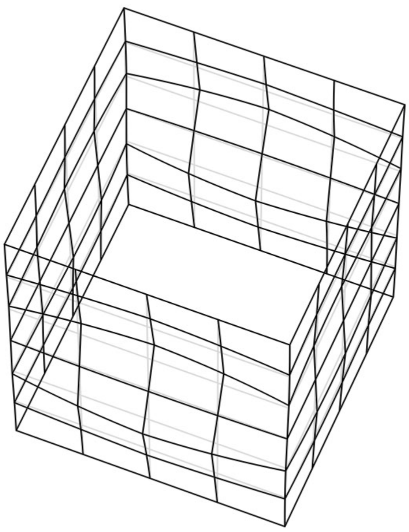

Fig. 14. The fifth stability eigenmode

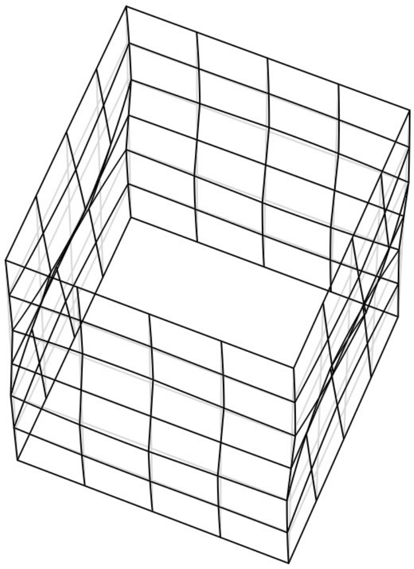

Fig. 15. The sixth stability eigenmode.

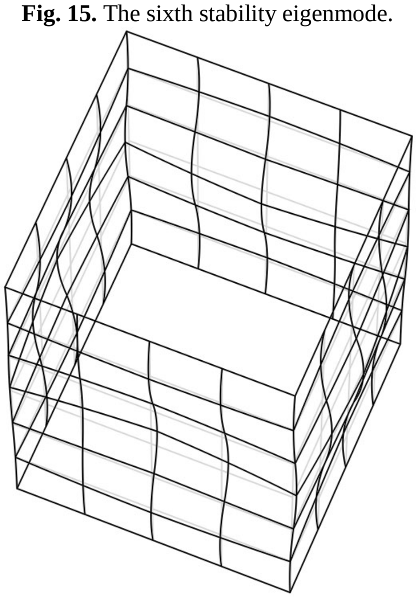

Fig. 16. The seventh stability eigenmode.

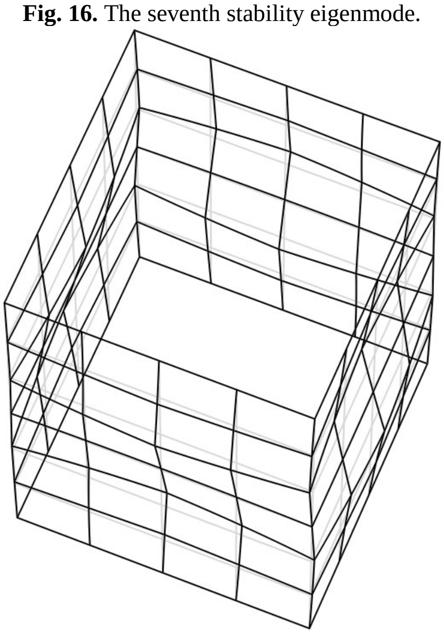

Fig. 17. The eighth stability eigenmode

Experimental investigation

Experimental investigation was performed by using the sample packages of two different sizes, the general views of which are presented in Fig. 18. In this paper the wording „machine direction of production“ means that the direction of production of the paperboard of the side walls during the process of production of the paperboard of the corresponding tested package is parallel to the vertical axis of the package, while the wording „cross-machine direction of production“ is used when the direction of production of the paperboard of the side walls of the package is perpendicular to the vertical axis of the package. The relationships of dependence of deformations on the compression force were obtained by performing the experiments of compression of empty boxes.

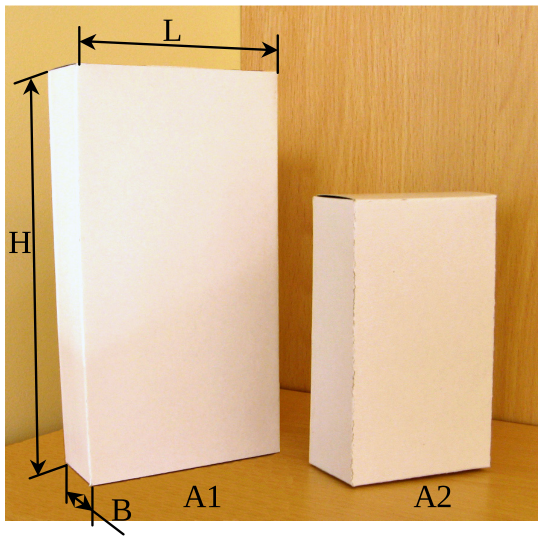

a)

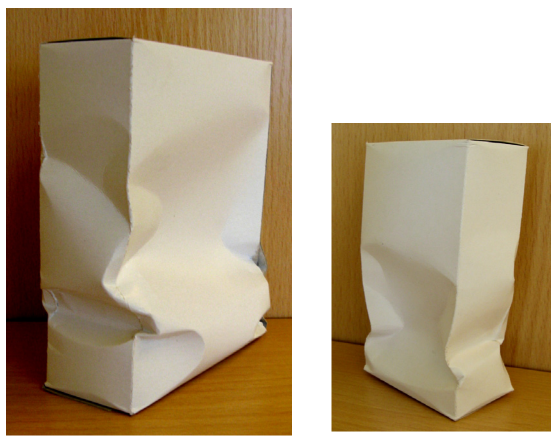

A1 A2

b)

Fig. 18. Examples of sample packages: a) before deformation: A1) box of size I (H= 230 mm, L= 118 mm, B= 48 mm), A2) box of size II (H=137 mm, L= 77 mm, B= 37 mm); b) after deformation

Technical characteristics of the paperboard used in experimental investigations are presented in Table 1.

Table 1

Technical characteristics of Paperboard Mirabell

Properties	Paperboard Mirabell
Grammage, g/m^2	400
Thickness, μm	580
Stiffness, L&W[1], Nm (5°) MD[3] CD[4] $\sqrt{MD \times CD}$	 60,9 24,4 38,5
Stiffness, TABER[2], Nm (15°) MD[3] CD[4] $\sqrt{MD \times CD}$	 28,9 10,9 17,8

Moment measured by the device L&W[1]*, which is necessary for bending of the sample of material by an angle of 50°*
Moment measured by the device TABER[2]*, which is necessary for bending of the sample of material by an angle of 150°*
[3] *- MD (machine direction) longitudinal direction of production of paperboard*
[4] *- CD (cross machine direction) transverse direction of production of paperboard*

For experimental testing a setup for the compression of boxes was used. The simplified diagram of the setup is presented in Fig. 19.

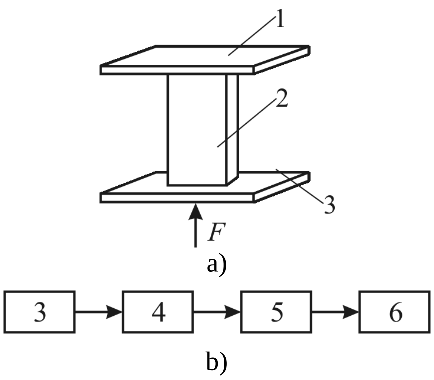

Fig. 19. Equipment for experimental investigation: a) diagram of compression of packages: 1 – upper supporting plate, 2 – the compressed package, 3 – lower supporting plate of the setup for the analysis of compression with attached tensoconverters, *F*, N – the vertical load; b) structural diagram for the measurement of deformations: 4 – the tensometric amplifier TS – 3, 5 – oscilloscope PicoScope 3424, 6 – monitor of the personal computer

The investigated packages 2 during the experiments were put on the lower supporting plate 3, which has the tensoconverters mounted on it. The previously mentioned plate 3 is connected with the tensoresistor measurement block. During the experiments with packages the electrical signal obtained from the sensor system was amplified by the tensometric amplifier TS – 3 (position 4). The obtained analogue signal was transferred to the oscilloscope PicoScope 3424 (position 5) for the conversion to the digital signal. The relationship between the compression force and the deformations was observed in the monitor of the personal computer 6. During the experiment the lower support of the setup was moving with the constant velocity of $3{,}5\times10^{-4}$ m/s in the vertical direction upwards, the upper part of the package contacted the immovable upper supporting plate and the process of compression of the package started.

The obtained results of experimental investigation of compression of packages are presented in Fig. 20.

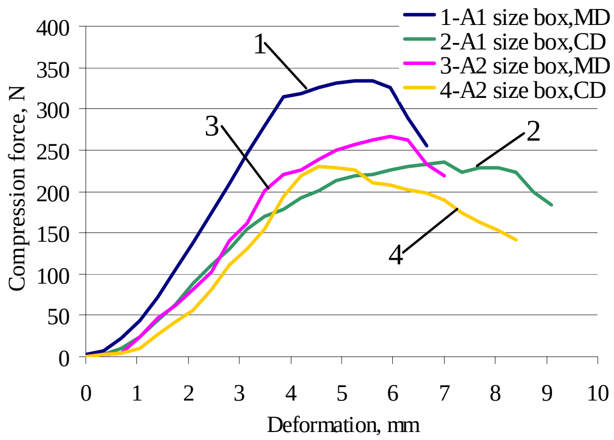

Fig. 20. Graphical relationships of resistance to compression of boxes produced from the paperboard Mirabell 400 g/m^2: 1 – box of size A1 (machine direction); 2 – box of size A1 (cross-machine direction); 3 – box of size A2 (machine direction); 4 – box of size A2 (cross-machine direction)

From the graphical relationships presented in Fig. 20 it may be observed that the boxes of size A1 produced from the paperboard of 400 g/m^2 in the machine direction of production resist the maximum loading, which reaches 328,6 N (for the axial deformation of 5,6 mm) – see the curve 1. The direction of production of paperboard has influence to the strength of the box. The boxes of paperboard 400 g/m^2 for the cross-machine direction of production of paperboard resist the 30% lower load (up to 235,47 N), with the axial deformation of 7 mm (see the curve 2).

The box of type A2 produced from the paperboard of 400 g/m^2 with the machine direction of production with the deformation of 5,6 mm resists the loading up to 267,56 N (see the curve 3). And the same box produced from the paperboard of 400 g/m^2 with the cross-machine direction of production of paperboard resists the loading force, which is 15% lower (up to 228,09 N), and the deformation starts from 5,95 mm (the curve 4).

Conclusions

The model for the analysis of stability of a long structure with a constant thin-walled cross-section was developed.

Stability of the structure with the square cross-section because of the additional stiffness due to the static compression was studied and the first stability eigenmodes were determined.

The problem for the analysis of stability of a shell-type structure is based on the assumption that a structure has additional stiffness due to its static compression.

The static problem was solved by assuming that the displacements at the edges of the analyzed structure are given. Then the stability of the structure subjected to additional stiffness (due to the static compression determined previously) was analyzed.

In the process of experimental investigation the maximum compressive loading was determined. When this loading is exceeded substantial deformations of the package are generated.

The packages of any size produced from paperboard which has the direction of production of paperboard of the side walls perpendicular to the vertical axis of the package withstand lower compressive loading in comparison to packages, which have the direction of production of paperboard of the side walls parallel to the vertical axis of the package. However, the deformation of the packages of the first type is larger.

The results of the presented numerical analysis are applicable in the range of elastic deformations and enable to investigate the main features of the process of compression of packages.

The results of the presented experimental and numerical study are applied in the design of packages.

References

[1] **Zienkiewicz O. C.** The Finite Element Method in Engineering Science. Moscow: Mir, 1975.

[2] **Kibirkštis E., Lebedys A., Kabelkaitė A., Havenko S.** Experimental study of paperboard package resistance to compression // Mechanika / Kaunas Technological University, Lithuanian Academy of Sciences, Vilnius Gediminas Technical University. - ISSN 1392-1207. - Kaunas. - 2007, vol. 1 (63), p. 27-33.